

Electronic Supplementary Information

Photocatalytic H₂O₂ production with perylene(bis-imide)-doped periodic mesoporous silica using micropollutants as sacrificial donors

Charlotte David, Stephane Grolleau, Denys Grekov, Aydar Rakhmatullin, Errol Blart, Valerie Hequet,* Yann Pellegrin*

I. General

Chemicals were purchased from Sigma-Aldrich, Fisher Scientific or Sodipro and used as received. Dialysis cassettes were purchased from Fisher Scientific. Thin-layer chromatography (TLC) was performed on aluminum sheets precoated with Merck 5735 Kieselgel 60F254. Column chromatography was carried out with Merck 5735 Kieselgel 60F (0.040-0.063 mm mesh). ¹H spectra were recorded on an AVANCE 300 UltraShield BRUKER. Chemical shifts for ¹H NMR spectra are referenced relative to residual protium in the deuterated solvent (CDCl₃ δ = 7.26 ppm). NMR spectra were recorded at room temperature, chemical shifts are written in ppm and coupling constants in Hz. Mass spectrometry was performed with a JEOL JMS-700 B/E spectrometer. Ultrafiltration was performed with centrifugal filter units from Millipore (100 kDa cutoff).

UV-visible absorption spectra were recorded on an Analytik Jena spectrophotometer, using 1 cm path length cells. Emission spectra were recorded on a Fluoromax-3 Horiba spectrofluorimeter (1 cm quartz cells). Luminescence decays were recorded with a DELTAFLEX time correlated single photon counting system (HORIBA).

The size of the nanoparticles was measured by transmission electron microscopy (TEM) using a JEOL 1230 operating at 80 kV. Samples were prepared by drop casting nanoparticles suspensions on copper TEM grids. The dried grids were then irradiated in a UV Ozone cleaner during 30 minutes (Nanobioanalytics - UVC-1014). Before measuring nanoparticles Feret diameters, TEM images were segmented using StarDist model deep learning method. The model supplied by Uwe Schmidt et al ¹ were learnt with a bank of 11 TEM images and their segmented relatives.

Solid-state MAS NMR spectra were measured at 9.4 T using a Bruker AVANCE III HD spectrometer with 4 mm probe. The ¹H-¹³C and ¹H-²⁹Si cross-polarization (CP) MAS NMR spectra were recorded at a spinning frequency of 10 and 14 kHz using a ramped cross-polarization with a recycle delay of 0.5 s and a contact time of 1 and 2 ms, respectively. ¹H decoupling was achieved using the SPINAL-64 sequence with a ¹H nutation frequency of about

60 kHz. Chemical shift is referred to TMS. All MAS NMR spectra were modeled using the Dmfit program.²

The infrared spectrometer used for this study was an IRTF Bruker device, alpha II, equipped with a "rock-solid" interferometer and a middle source. The used spectral resolution was 4 wavenumbers and the spectra were recorded in an ATR mode and resulted from 200 accumulations. The used software to treat spectra is OPUS 7.5. version.

XPS analysis were performed on a K Alpha+ spectrometer (ThermoFisher), equipped with a monochromated X-Ray Source (AlK α , 1486.6 eV). An X-ray spot size of 400 μ m was used. The hemispherical analyzer was operated in CAE (Constant Analyzer Energy) mode, with a pass-energy of 100 eV and a step of 1 eV for the acquisition of survey spectra, while a pass-energy of 40 eV and a step of 0.1 eV were used for the acquisition of high resolution spectra. The spectra were recorded and data processing was performed with Advantage[®] software (V 5.99 from ThermoFisher). The elemental surface compositions were calculated by determining the area of each element of interest with a Shirley type background subtraction and using the Scofield sensitivity factors of the spectrometer. The spectra were calibrated against the C1s main peak component C-C/C-H set at 285.0 eV.

UV-visible absorption spectra were recorded on an Analytik Jena spectrophotometer, using 1 cm path length cells. The steady-state fluorescence spectra were recorded on a Horiba Fluoromax-4 spectrofluorimeter (1 cm optical path quartz cells). Luminescence decays were recorded with a Horiba DELTAFLEX TC-SPC. The energy of the excited state of the dye PDI1 E⁰⁰ was estimated by retrieving the wavelength at the intersection between the normalized absorption and emission spectra.

The photocatalysis was performed with a green EvoluChem[™] LED spotlights (525 nm, 18W) into an HepatoChem EvoluChem[™] PhotoRedOx Box. In a typical experiment, a solution of pollutant was prepared in distilled water. To a vial containing a known weight (between 2.5 and 3.5 mg) of photoactive material were added 1 mL of previous pollutant solution per milligram of photoactive material. The vial was then irradiated during 8 hours under air in the PhotoRedOx Box. The concentration of H₂O₂ was estimated by a colorimetric method using leuco-crystal violet (LCV) as colorimetric indicator in presence of Horseradish peroxidase (HRP). The H₂O₂ photoproduction rate was calculated as the number of micromoles per litre and per hour (over 8 hours experiment).

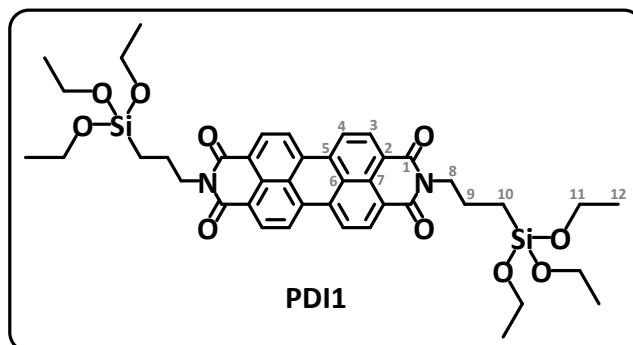
Nitrogen physisorption was used for textural analysis of the synthesized materials. Prior to isotherm measurement, samples were outgassed overnight under dynamic secondary vacuum at 150 °C. N₂ adsorption and desorption isotherms were measured at 77 K (liquid nitrogen bath) in a fixed increment mode using 3Flex automated adsorption analyser from

Micromeritics. Volumes of sample cells unoccupied by the solid were measured by He expansion at ambient temperature and at 77 K. Specific surface area was determined from the results of isotherm modelling with Brunauer Emmett Teller (BET) equation in pressure range adjusted according to IUPAC recommendations.³ The distribution of mesopore sizes was determined by NLDFT modelling of adsorption branches with the kernel for cylindrical pores⁴ (case of oxide surface).

The studies of the adsorption of pollutants on the porous silica material were performed as follows: the pollutants and the PDI-SiO₂ material were brought together in water (pH 6.5) and after equilibration (five days) the solutions were filtrated and the quantities of remaining pollutant (C_e in mg/L) were estimated by UV-Vis spectroscopy. Quantities of pollutants adsorbed on PDI-SiO₂ (q_e in mg/L) are deduced by mass balance.

II. Synthesis

1) Synthesis of N,N-bis-(3-(triethoxysilyl)propyl)perylene-3,4,9,10-tetracarboxy-dianhydride (PDI1)



In a dry schlenk under argon were added perylene-3,4,9,10-tetracarboxy-dianhydride (1.3 mmol, 500 mg, 1 eq) and 3-(triethoxysilyl)propan-1-amine (15.4 mmol, 3.6 mL, 12 eq). The reaction mixture was stirred at room temperature until homogeneous then stirred for 3 h at 130°C. After cooling, the crude mixture was diluted with dichloromethane, filtered and concentrated. The crude product was purified by chromatography column (SiO₂, dichloromethane). Two fractions were retrieved: the first one was a dark shade of red and was first collected as a crystal clear solution. After evaporation under reduced pressure, a dark red powder of polymeric material was obtained, which proved insoluble in all solvents or solvents mixtures available in our laboratory. The second fraction was light a red solution which upon concentration under reduced pressure gave PDI1 as a stable red powder.

Characterization of PDI1:

¹H NMR (300 MHz, CDCl₃): δ (ppm) = 8.63 (d, J = 8.0 Hz, 4H, H₃), 8.53 (d, J = 8.0 Hz, 4H, H₄), 4.20 (massif, 4H, H₈), 3.83 (q, J = 7.0 Hz, 12H, H₁₁), 1.88 (massif, 4H, H₉), 1.23 (t, J = 7.0 Hz, 18H, H₁₂), 0.78 (massif, 4H, H₁₀)

¹³C NMR (75 MHz, CDCl₃): δ (ppm) = 163.4 (C₁), 134.6 (C₅), 131.5 (C₃), 129.4 (C₇), 126.5 (C₆), 123.4 (C₂), 123.1 (C₄), 58.6 (C₁₁), 43.2 (C₈), 21.7 (C₉), 18.4 (C₁₂), 8.2 (C₁₀)

MS (ASAP+): calcd for C₄₂H₅₀N₂O₁₀Si₂ 798.3004, found 798.2991

2) Synthesis of PDI-SiO₂ material

PDI-SiO₂ was synthesized as follows: in a 20 mL vial were added PDI1 (0.098 mmol, 78 mg, 2%mol), CTABr (0.59 mmol, 215 mg, 12 %mol) and dichloromethane (10 mL). The mixture was stirred until homogeneous then slowly concentrated. The obtained dried powder was ground in a mortar. The obtained fine powder was introduced in a Schlenk then water (10 mL) and ethanol (2.3 mL) were added and the mixture was stirred until homogeneous. Tetraethoxysilane (4.93 mmol, 1.1 mL, 1 eq) and NH₃ 25% (2.9 mL) were finally added and the reaction mixture was stirred, first for 1h at room temperature, then without stirring, for 4 days

at 90°C. After cooling, the crude powder was filtered and washed several times with water, ethanol and dichloromethane. The structure-directing agent CTABr was removed by washing in hot acidic ethanol according to the literature.⁵ The resulting material was then washed with ethanol and dried to afford a pink powder of PDI-SiO₂.

Characterization of PDI-SiO₂ (MAS solid-state NMR):

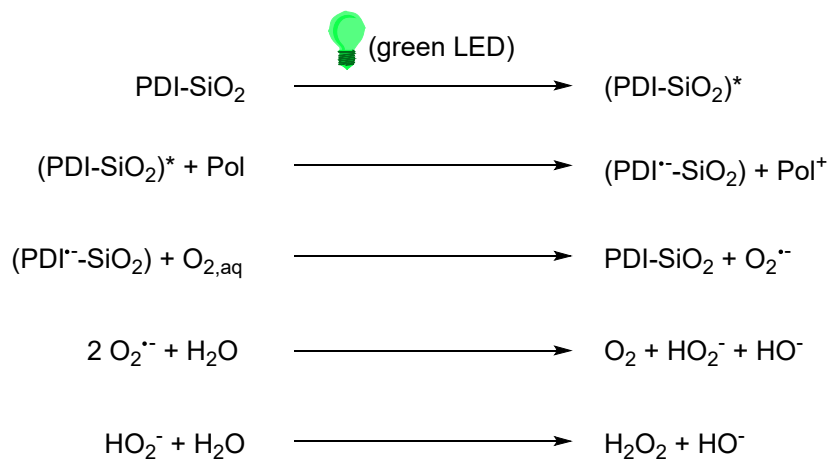
¹³C NMR (14 kHz): δ (ppm) = 163.4, 133.2, 128.6, 122.5, 58.2, 44.1, 21.9, 10.2.

²⁹Si NMR (8 kHz): δ (ppm) = -47.1, -58.5, -67.0, -91.5, -100.6, -110.7.

III. Detailed procedure for the estimation of the concentration of H₂O₂ in photolyzed mixtures:

A 0.74 mM aqueous solution of Leuco Crystal Violet (LCV) was prepared by dissolving 50 mg of LCV into a solution of 79.6 mL of water and 0,4 mL of 37% HCl ([HCl] \approx 5% in volume). The previous mixture was then added into a solution of 95.5 mL of water and 0.5 mL of HCl (37%). In parallel, a 1 mg.mL⁻¹ HRP solution was prepared. The titration of H₂O₂ was then realized by adding successively 250 μ L of the LCV solution, 20 to 50 μ L of the photolyzed solution, 125 μ L of HRP solution, 2 mL of acetate buffer (ABCR, AB354653: 1 M, pH = 5.0) and 1.5 mL of milliQ water. A blue color appears after the addition of HRP solution and turns to a violet color after the addition of buffer (maximum absorbance at 592 nm). The concentration of H₂O₂ for all samples was estimated by measuring the absorbance at 592 nm of the previous mixture, and comparing with a calibration curve prepared in the same conditions with solutions of known H₂O₂ concentration (calibration realized with prepared samples where [H₂O₂] ranged from 1.5 to 25 μ M).

IV. Schemes and Figures



Scheme S1. Mechanism of H₂O₂ production from mixtures of PDI-SiO₂, pollutants (pol) in water under light soaking.

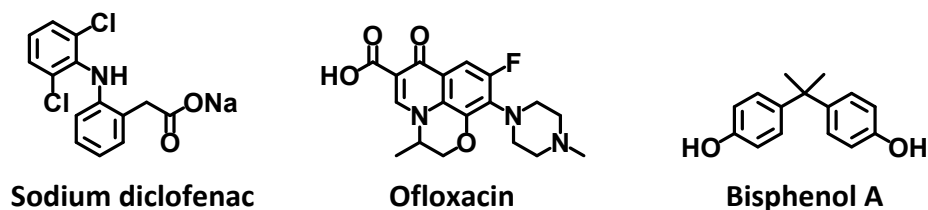


Figure S1. Molecular structures of the pollutants used in this study: sodium diclofenac, ofloxacin and BPA.

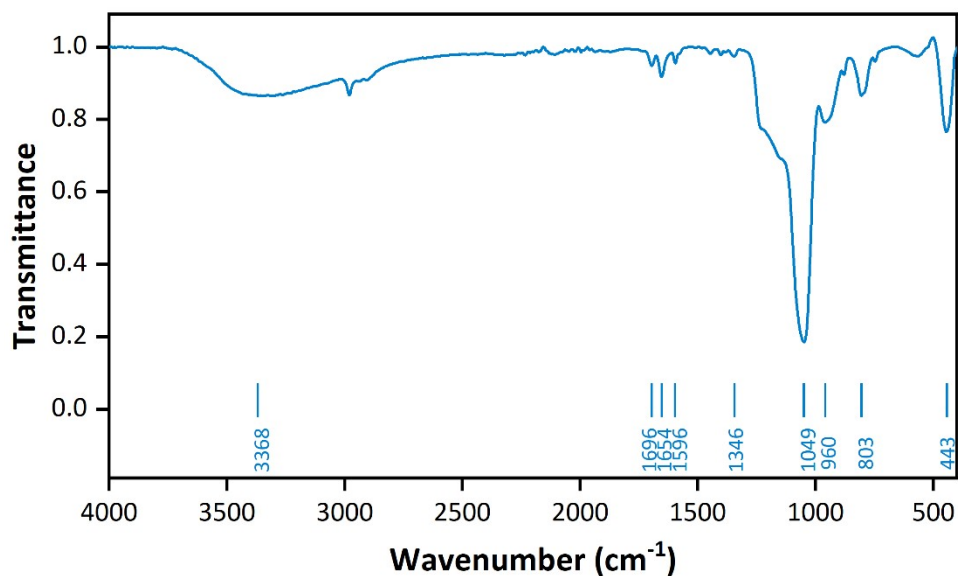


Figure S2. FTIR spectrum of PDI-SiO₂.

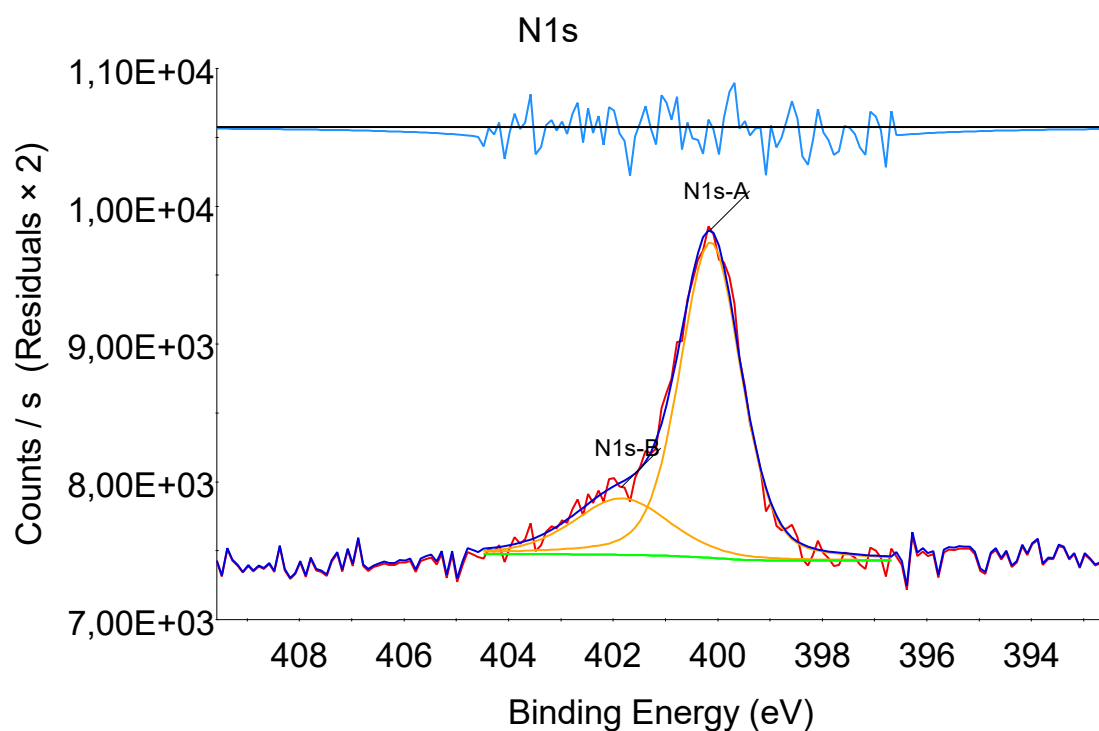


Figure S3. Peak fitting for N1s. Two populations of nitrogen atoms were observed, N1s-A (neutral N) and N1s-B (charged N). Charged nitrogen atoms are associated to remnant CTAB (N_{CTAB} , 22% of the total nitrogen atoms population). Neutral nitrogen atoms are associated to PDI (N_{PDI} , 78%). Measured molar percentages for N_{total} and Si are 1.02% and 24.71% respectively, leading to $\%(\text{NPDI}) = 0.8\%$. The molar ratio between PDI and SiO_2 is thus $0.4 / 24.71 = 0.016$.

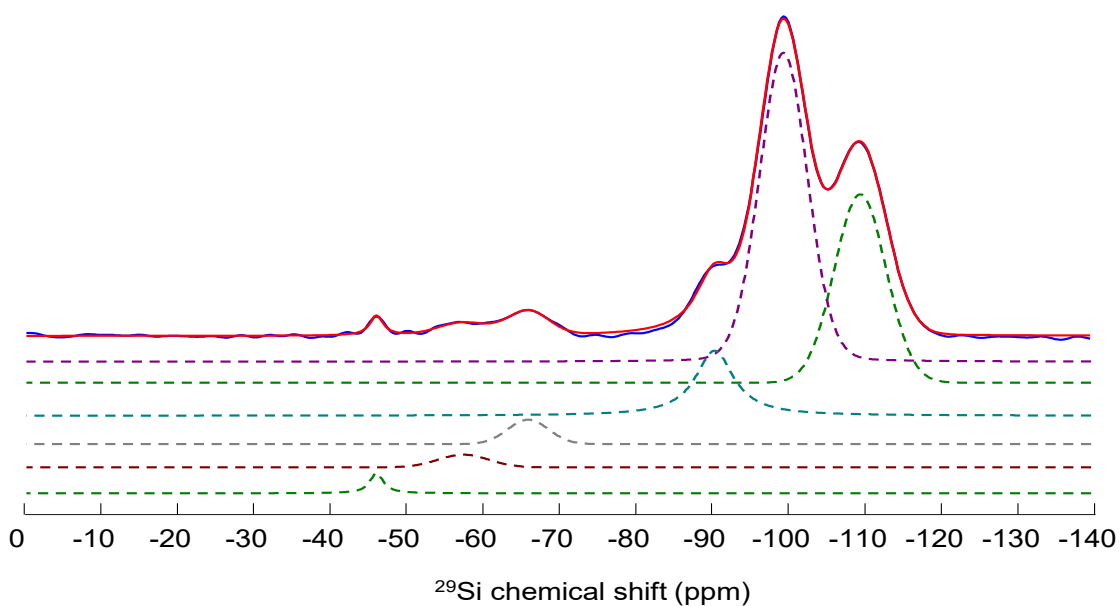


Figure S4. ^{29}Si CP-MAS NMR experimental (blue line) spectrum of PDI-SiO₂ at 9.4 T and its simulation (red line). Decomposition of the theoretical spectrum in its individual components (coloured dashed curves).

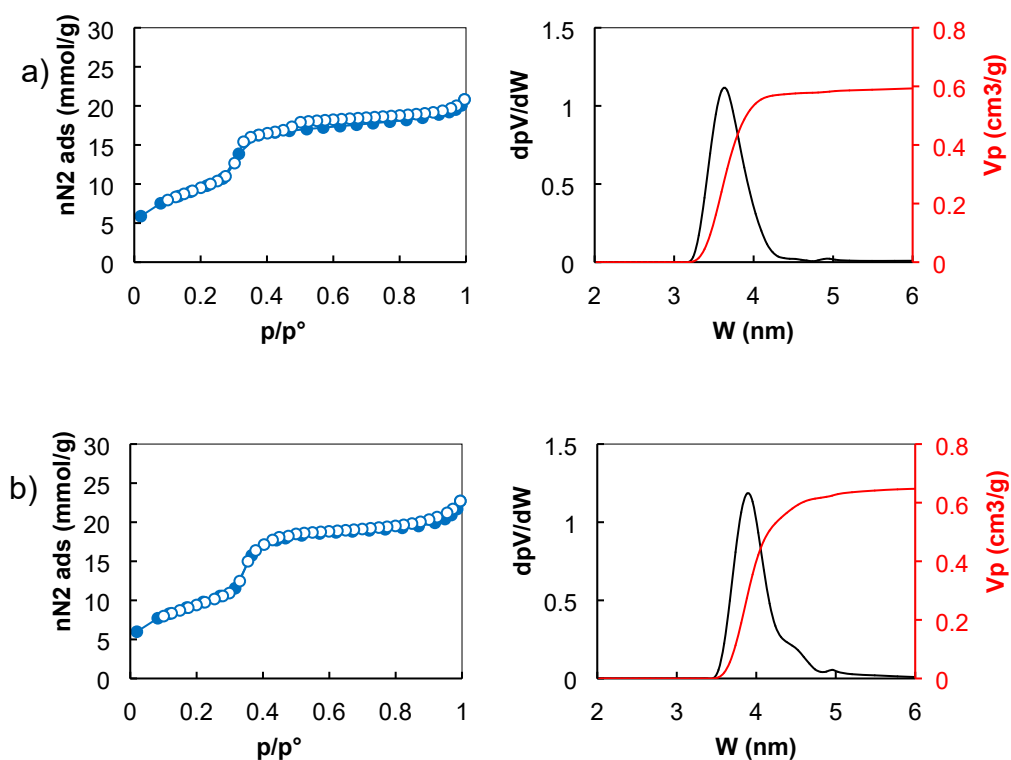


Figure S5. Nitrogen adsorption (filled symbols) and desorption (empty symbols) isotherms at 77 K for (a) u-SiO₂ and (b) PDI-SiO₂ materials together with corresponding pore size distribution determined by NLDFT.

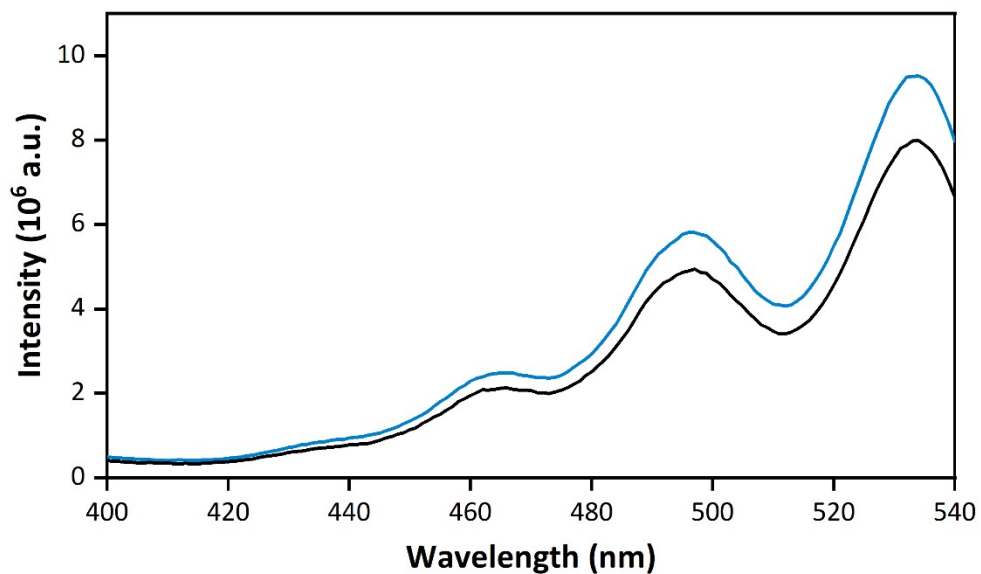


Figure S6. Excitation spectra of PDI-SiO₂ (species *A*) in aqueous suspension recorded for λ_{em} = 548 (blue line) and 593 nm (black line).

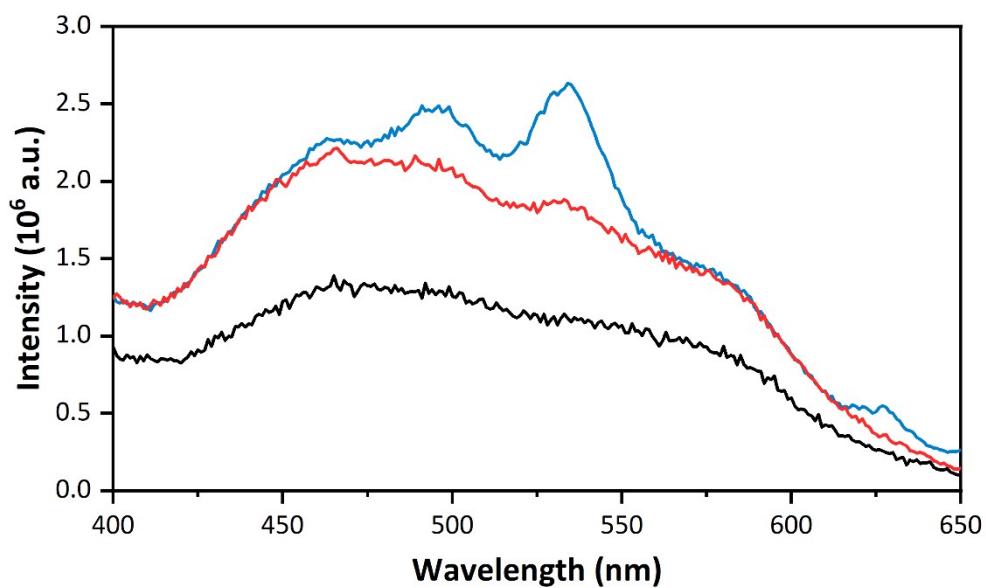


Figure S7. Excitation spectra of PDI-SiO₂ (species *B*) in aqueous suspension recorded for λ_{em} = 660 (blue line), 700 (red line) and 750 nm (black line).

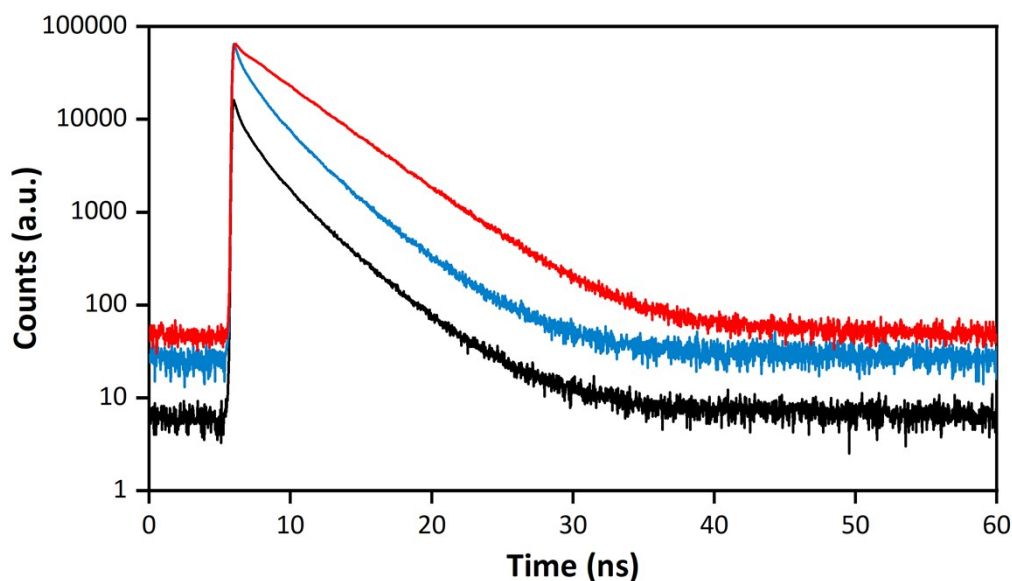
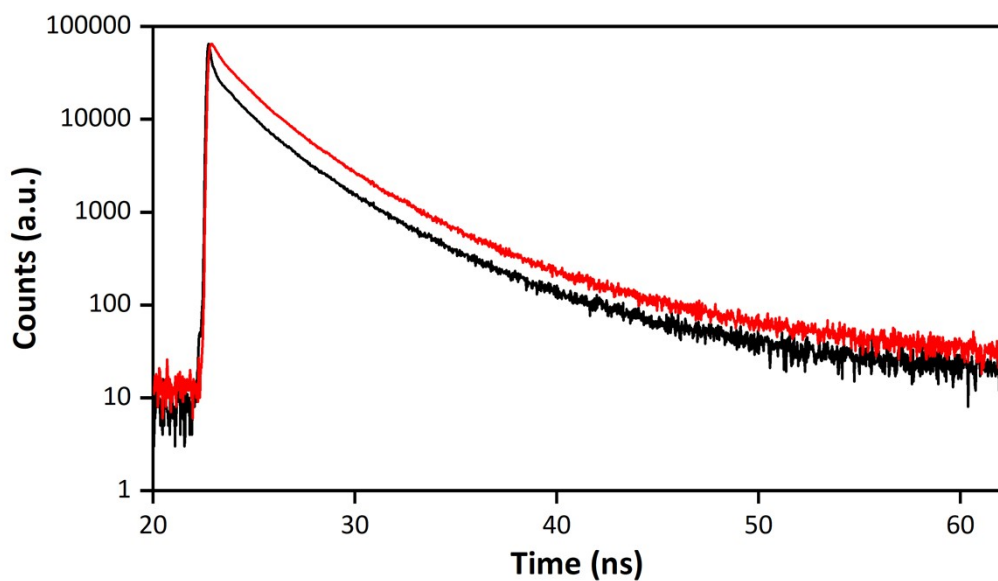


Figure S8. Emission decays of PDI1 (red line, 1 μM in dichloromethane, monitoring at 531 nm), PDI-SiO₂ species A (blue line, aqueous suspension, monitoring at 548 nm; black line, aqueous suspension, monitoring at 593 nm). Excitation at 438 nm.



Fit of the decay ($\chi^2 = 1.85$): 0.55 ns (16.9%); 2.31 ns (71.4%); 7.12 ns (11.8%)

Fit of the decay ($\chi^2 = 1.44$): 0.055 ns (15.9%); 0.82 ns (1.9%); 2.6 ns (57.6%); 8.46 ns (7.43%)

Figure S9. Emission decays of PDI-SiO₂ species B at $\lambda_{\text{em}} = 700$ nm (red line) and 750 nm (black line). Excitation with a delta diode laser at 438 nm. Lifetimes and relative contributions to the signal (in percentage) resulting from the best fitting of the data are given on the graphics.

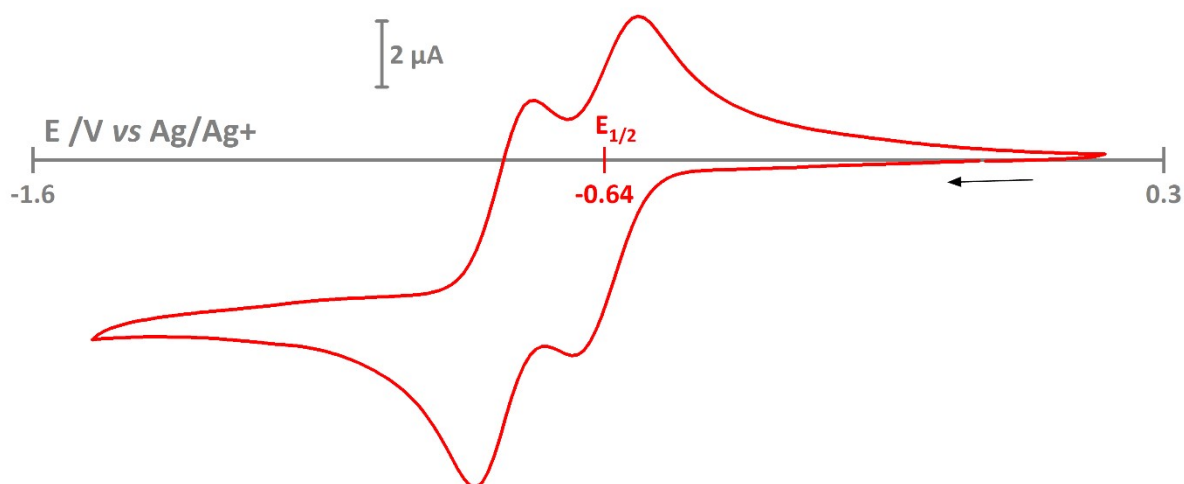


Figure S10. Cyclic voltammogram of PDI1 (1.25 mM) in dichloromethane (tetrabutylammonium hexafluorophosphate 0.1 M as supporting electrolyte). Working electrode: glassy carbon disk. Reference electrode: Ag/Ag⁺ in 0.1 M LiClO₄ in ethanol. Counter-electrode: platinum foil. Sweep rate at 100 mV.s⁻¹. The half wave potential for the first reduction wave was measured at $E_{1/2} = -1.06$ V vs. Fc⁺/Fc, which turns into ca. -0.55 V vs. SCE, assuming $E(\text{Fc}^+/\text{Fc}) = 0.51$ V vs. SCE.^{6,7} Knowing $E^{00} = 2.3$ eV (wavelength at the intersection between normalized absorption and emission spectra of PDI1 in CH₂Cl₂), the estimated value for $E(\text{PDI1}^*/\text{PDI1}^-)$ is 1.75 V vs. SCE in dichloromethane.

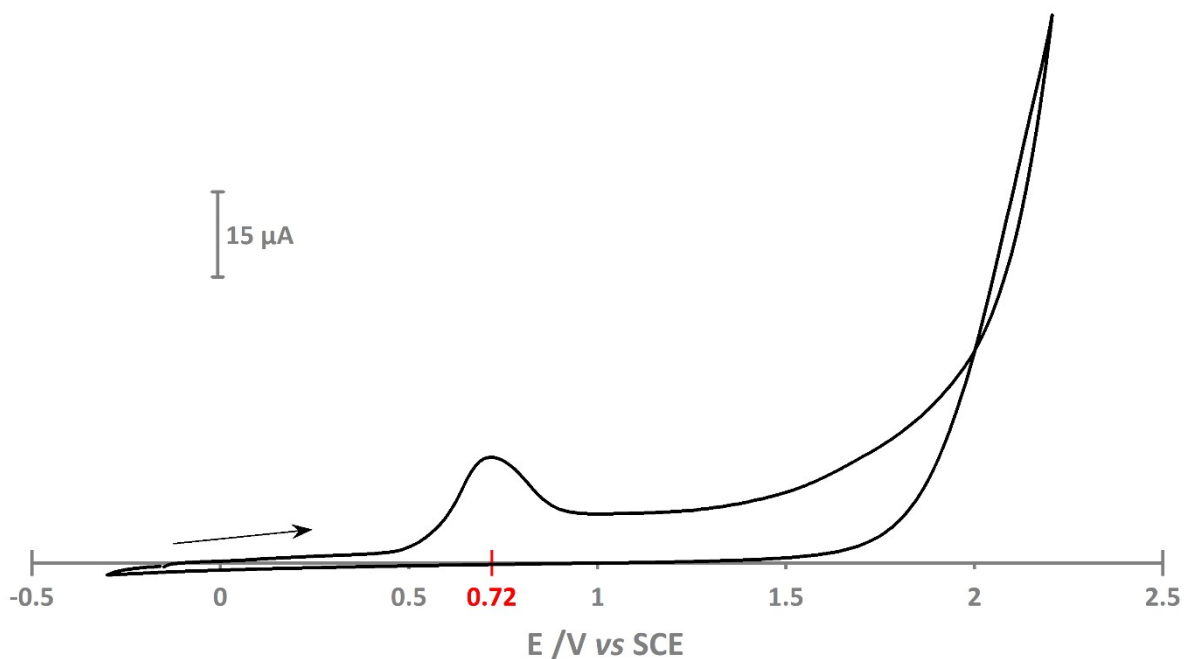


Figure S11. Cyclic voltammogram of diclofenac (0.8 mM) in water (LiCl 0.1 M as supporting electrolyte). Working electrode: glassy carbon disk. Reference electrode: Saturated Calomel Electrode (SCE). Counter-electrode: platinum foil. Sweep rate at 100 mV.s⁻¹.

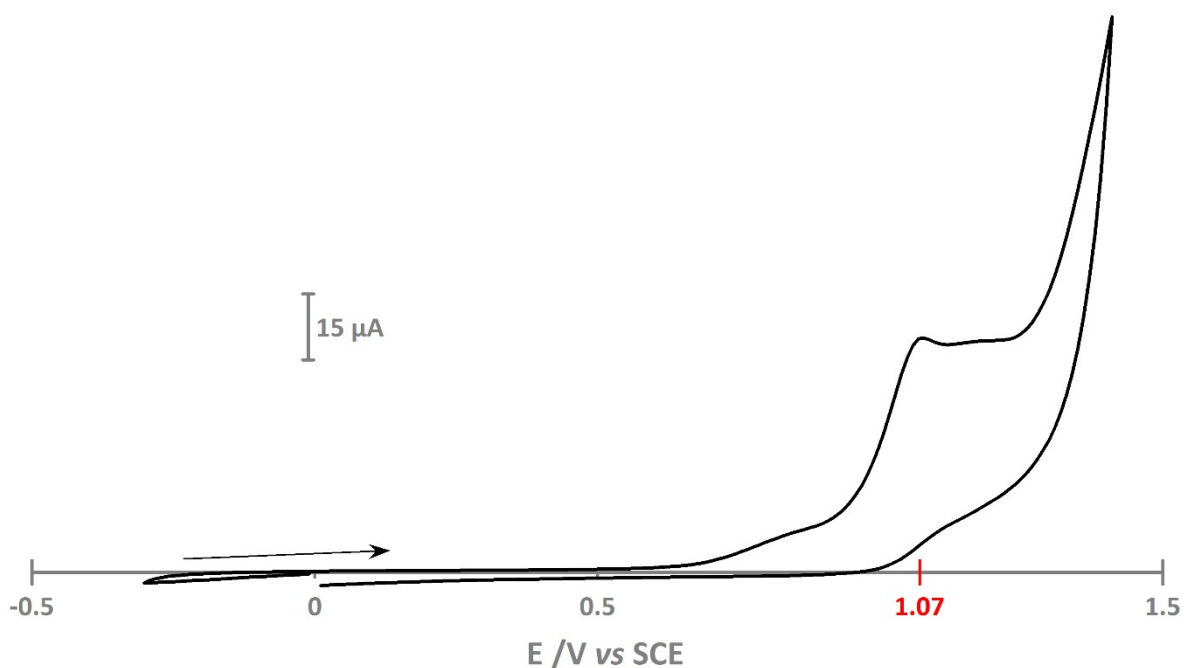


Figure S12. Cyclic voltammogram of ofloxacin (0.8 mM) in water (LiCl 0.1 M as supporting electrolyte). Working electrode: glassy carbon disk. Reference electrode: Saturated Calomel Electrode (SCE). Counter-electrode: platinum foil. Sweep rate at 100 mV.s⁻¹.

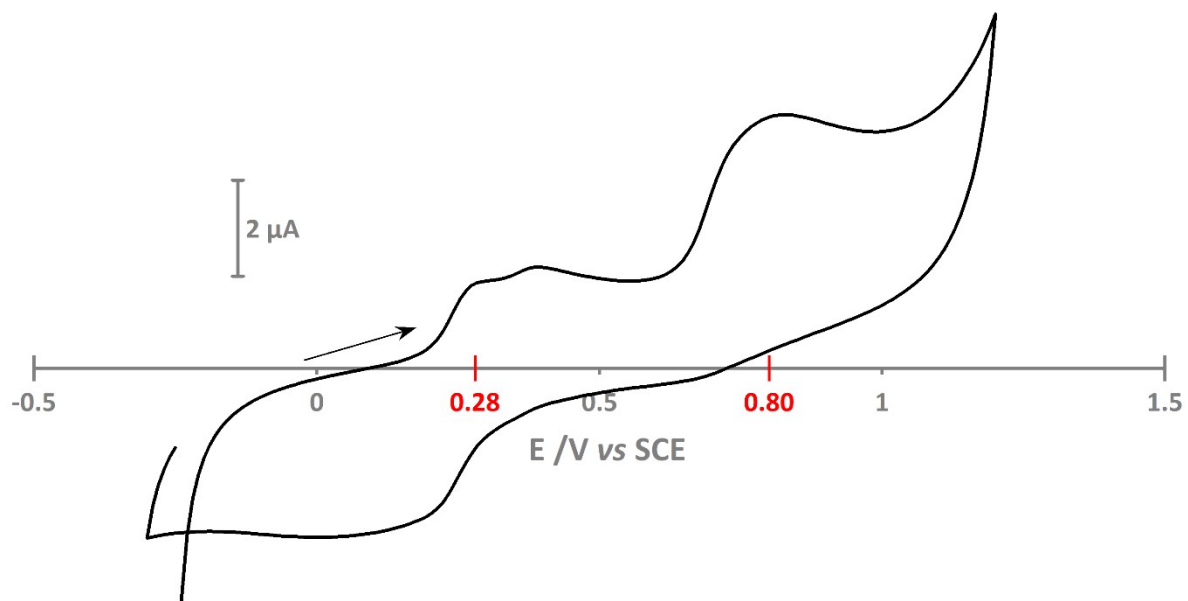


Figure S13. Cyclic voltammogram of BPA (0.2 mM) in water (LiCl 0.1 M as supporting electrolyte). Working electrode: glassy carbon disk. Reference electrode: Saturated Calomel Electrode (SCE). Counter-electrode: platinum foil. Sweep rate at 100 mV.s⁻¹.

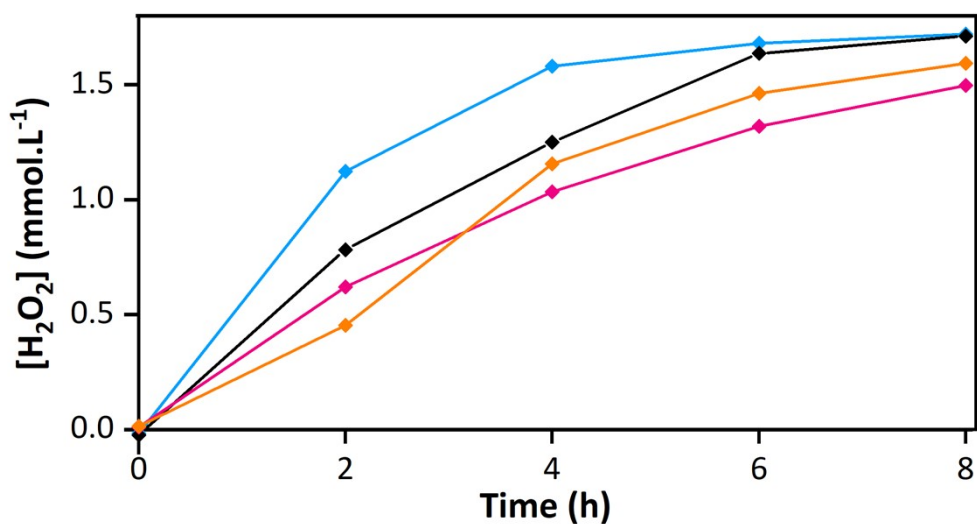


Figure S14. Photoproduction of H₂O₂ under 525 nm LED light with 1 mM ofloxacin in water. Black: standard conditions (1 mg.ml⁻¹ PDI-SiO₂, 1 mM ofloxacin, milliQ water, under air). Deviations from standard conditions: under pure O₂ instead of air (blue line), with 0.5 mg/mL PDI-SiO₂ instead of 1 mg/mL (pink line) and with tap water instead of milliQ water (orange line).

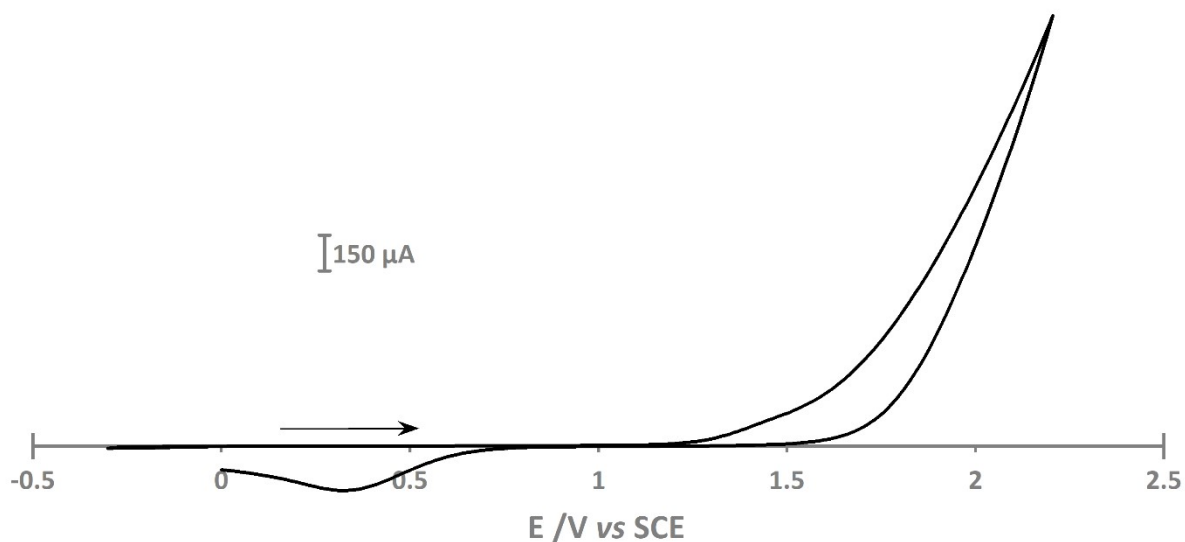


Figure S15. Cyclic voltammogram of glyphosate (1 mM) in water (LiCl 0.1 M as supporting electrolyte). Working electrode: glassy carbon disk. Reference electrode: Saturated Calomel Electrode (SCE). Counter-electrode: platinum foil. Sweep rate at 100 mV.s⁻¹.

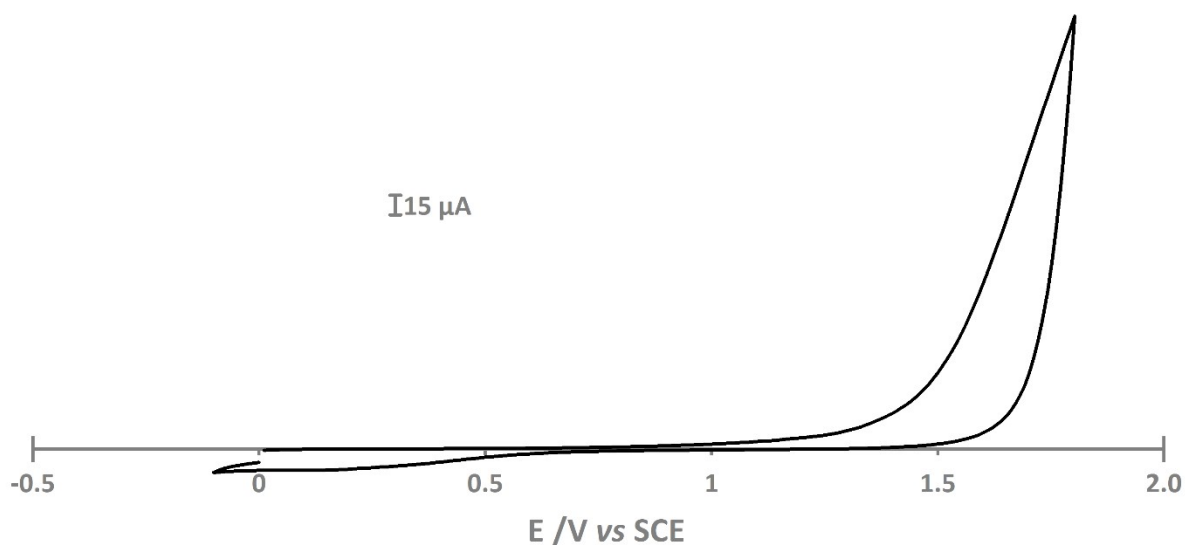


Figure S16. Cyclic voltammogram of metolachlor (1 mM) in water (LiCl 0.1 M as supporting electrolyte). Working electrode: glassy carbon disk. Reference electrode: Saturated Calomel Electrode (SCE). Counter-electrode: platinum foil. Sweep rate at 100 mV.s⁻¹.

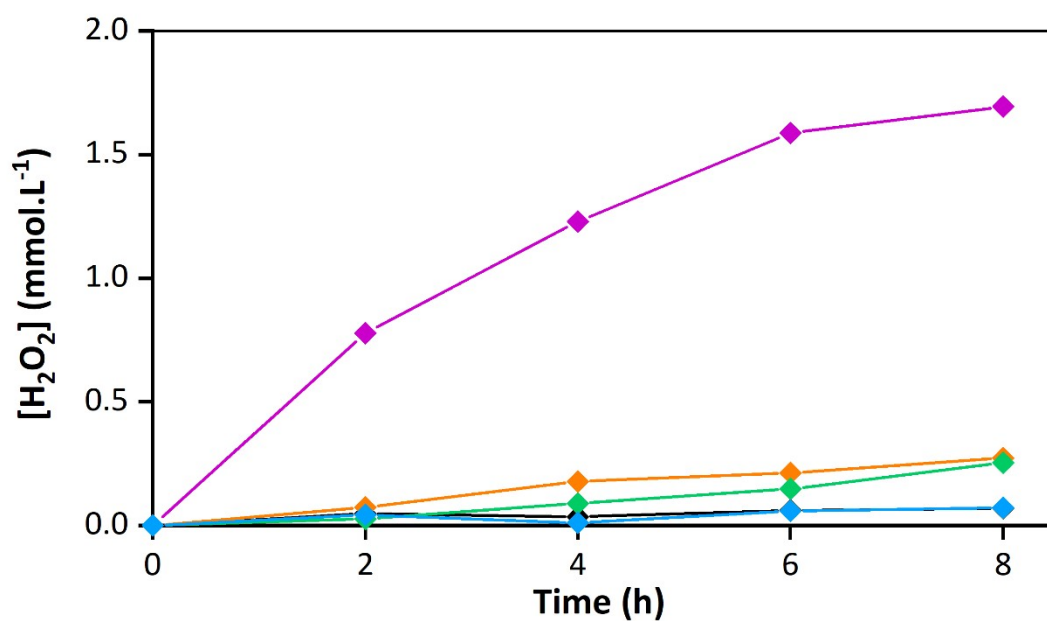


Figure S17. Photoproduction of H₂O₂ under 525 nm LED light with ofloxacin (1 mM, pink line), diclofenac (1 mM, orange line), BPA (1 mM, green line), glyphosate (1 mM, blue line) and

metolachlor (1 mM, black line) in water in standard conditions (1 mg.ml⁻¹ PDI-SiO₂, milliQ water, under air).

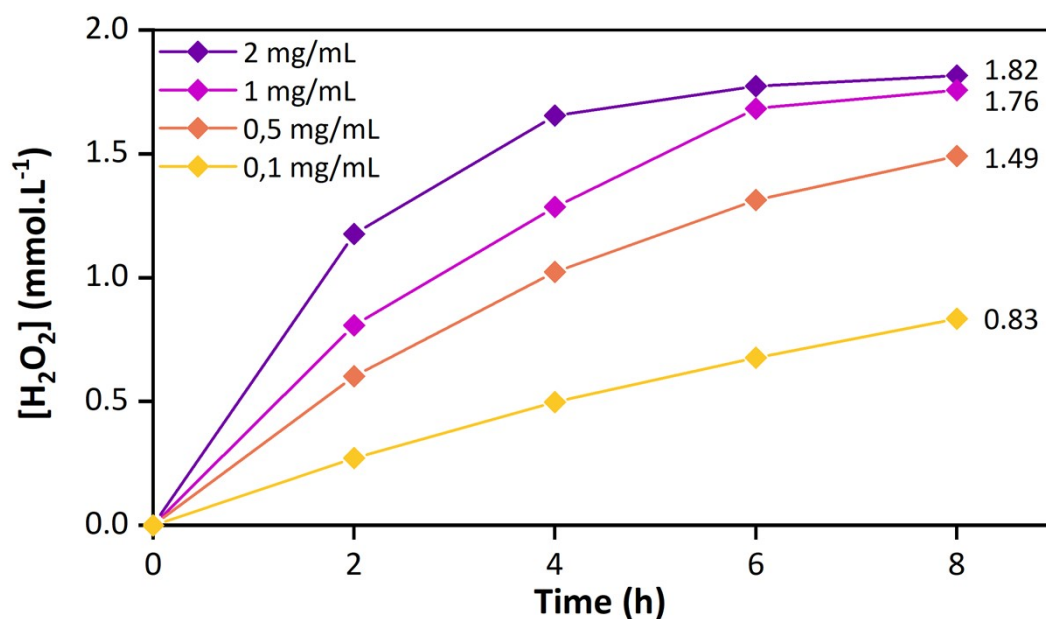


Figure S18. Influence of the loading in PDI-SiO₂ on the photoproduction of H₂O₂ (standard conditions, except the concentration in PDI-SiO₂: 0.1 mg/mL (yellow); 0.5 mg/mL (orange); 1 mg/mL (pink) and 2 mg/mL (purple)). Concentrations in H₂O₂ after 8 hours are given in mmol.L⁻¹ on the right side of the figure.

Table S1. Photogeneration of H₂O₂ in presence of sacrificial donors with a few selected heterogeneous photocatalysts.

entry	atmosphere	Photosensitive materials (quantities in mg/mL)	Sacrificial donor (concentration in mol.L ⁻¹)	[H ₂ O ₂] (mM)	rate (μM.h ⁻¹)	ref
1	O ₂ (1 atm)	TiO ₂ (10.0)	Benzyl alcohol (0.35)	39.6	3300	8
2	O ₂	gC ₃ N ₄	Ethanol	6.0	500	9

	(1 atm)	(4.0)	(90% in volume)			
3	O ₂ (1 atm)	Mesoporous C ₃ N ₄ (4.0)	Ethanol (90% in volume)	18.0	750	10
4	O ₂ (1 atm)	PDI/gC ₃ N ₄ (1.67)	H ₂ O	1.7	35	11
5	O ₂ (1 atm)	Aggregated PDI (0.25)	Oxalic acid (0.01)	n.r.	31	12
6	Air (1 atm)	PDI/gC ₃ N ₄ (1.0)	Isopropanol (10% in volume)	n.r.	85	13
7	Air (1 atm)	PDI-SiO ₂ (1.0)	Ofloxacin (0.001)	1.67	209	This work

Table S2. Photoproduction of H₂O₂ under 525 nm LED light with 1 mM ofloxacin in water, under air, over 24 hours, in presence of PDI-SiO₂ (1 mg.mL⁻¹) with additions of a fresh batch of ofloxacin every 8 hours. Δ[H₂O₂] is the amount of H₂O₂ produced over each 8-hour period.

Time (hours)	[H ₂ O ₂] (mM.L ⁻¹)	Δ[H ₂ O ₂] (mM.L ⁻¹)
8	1.75	-
16	3.40	1.65
24	5.20	1.80

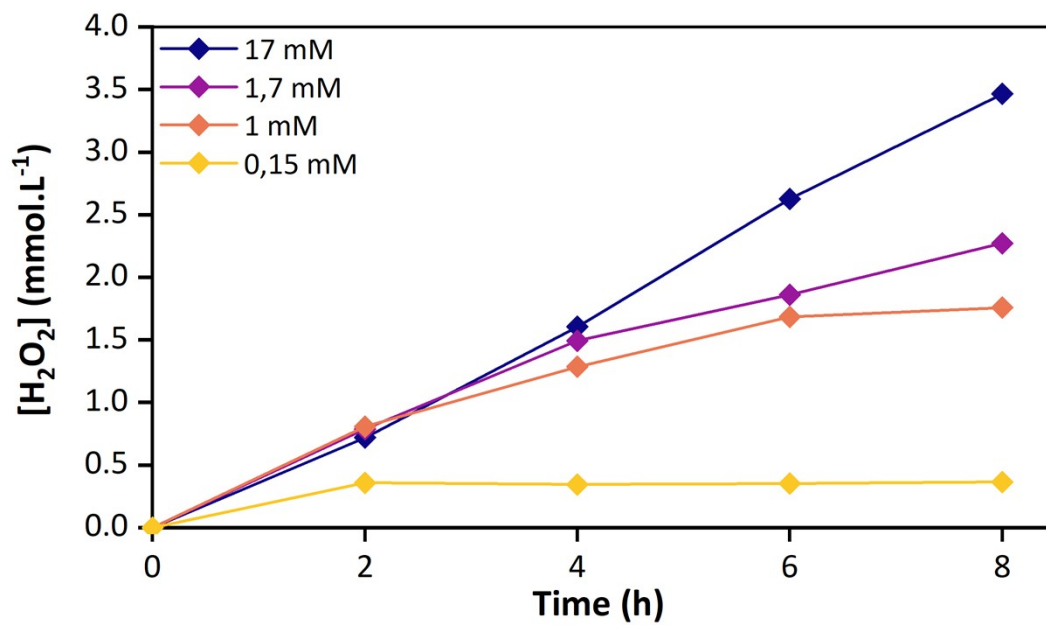


Figure S19. Dependence of H_2O_2 photo-production vs. the initial concentration in ofloxacin with a 1 mg/mL concentration of PDI-SiO₂ 2%

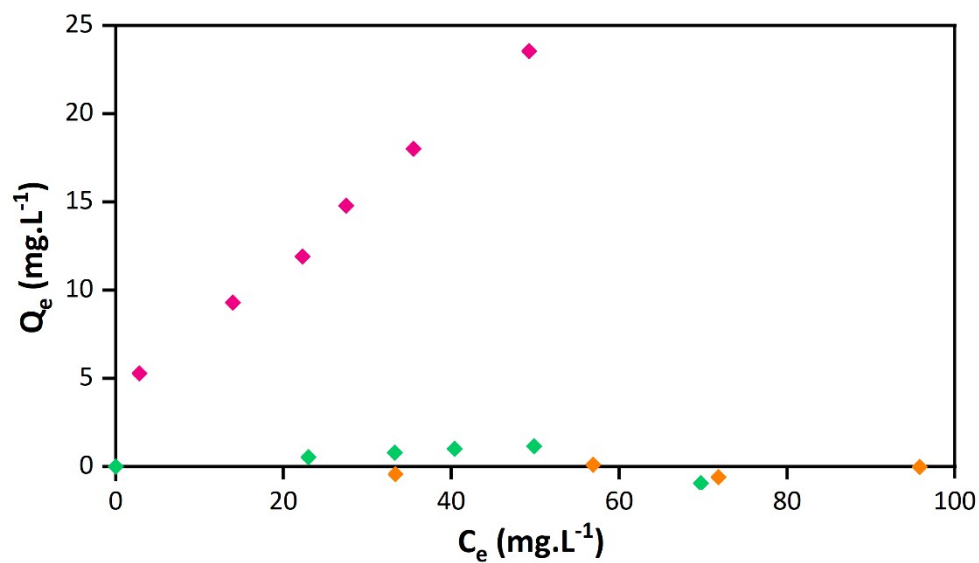


Figure S20. Summary of the adsorption of ofloxacin (pink dots), diclofenac (orange dots) and BPA (green dots) in PDI-SiO₂ in aqueous suspensions (pH = 6.5). Q_e = concentration of adsorbed pollutant; C_e = concentration of pollutant in the solution at equilibrium (the adsorption lasted 5 days to ensure equilibrium had been reached).

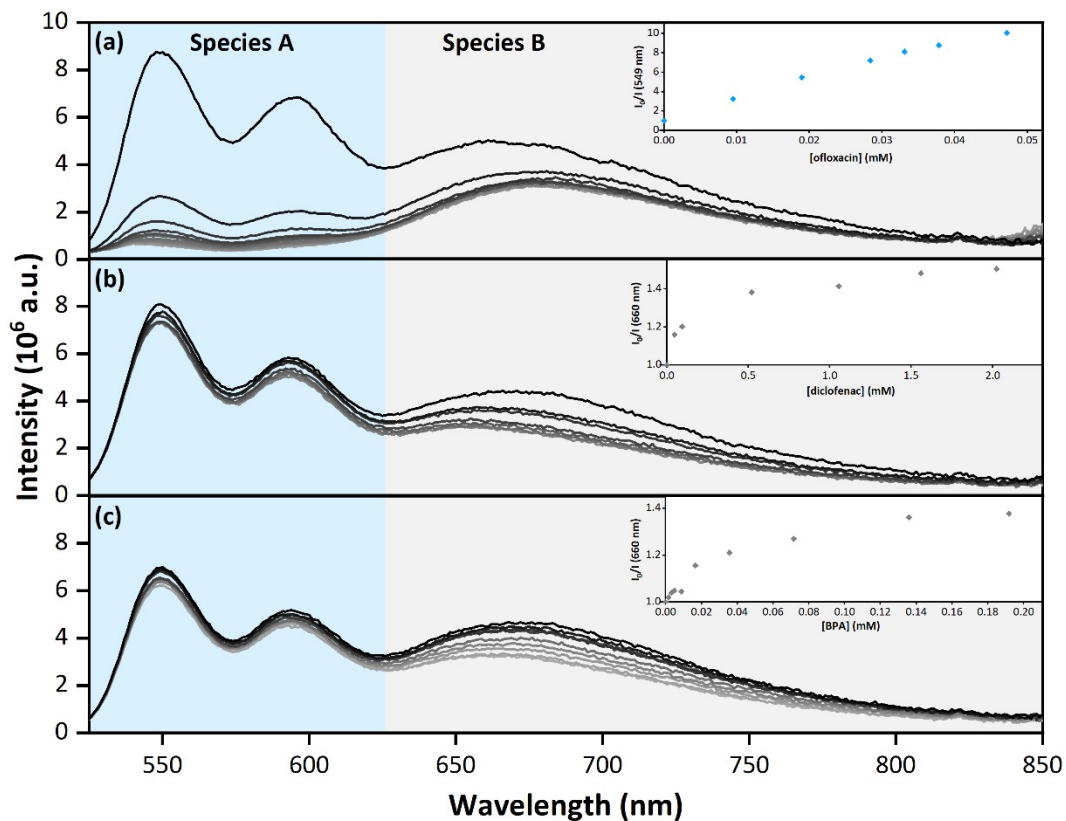


Figure S21. Stern-Volmer experiments for 1 mg/mL of PDI-SiO₂ in water in presence of (a) ofloxacin (from 0 to 60 mM), (b) diclofenac (from 0 to 2 mM) and (c) BPA (from 0 to 0.2 mM). Insets: Stern-Volmer plots $I_0/I = f([\text{pollutant}])$ where I_0 and I are the luminescence intensity in absence and in presence of pollutants respectively. Luminescence monitored at 549 nm (a) and 660 nm (b and c) by steady state fluorimetry. The concentration of BPA could not be increased above 0.3 mM for solubility reasons.

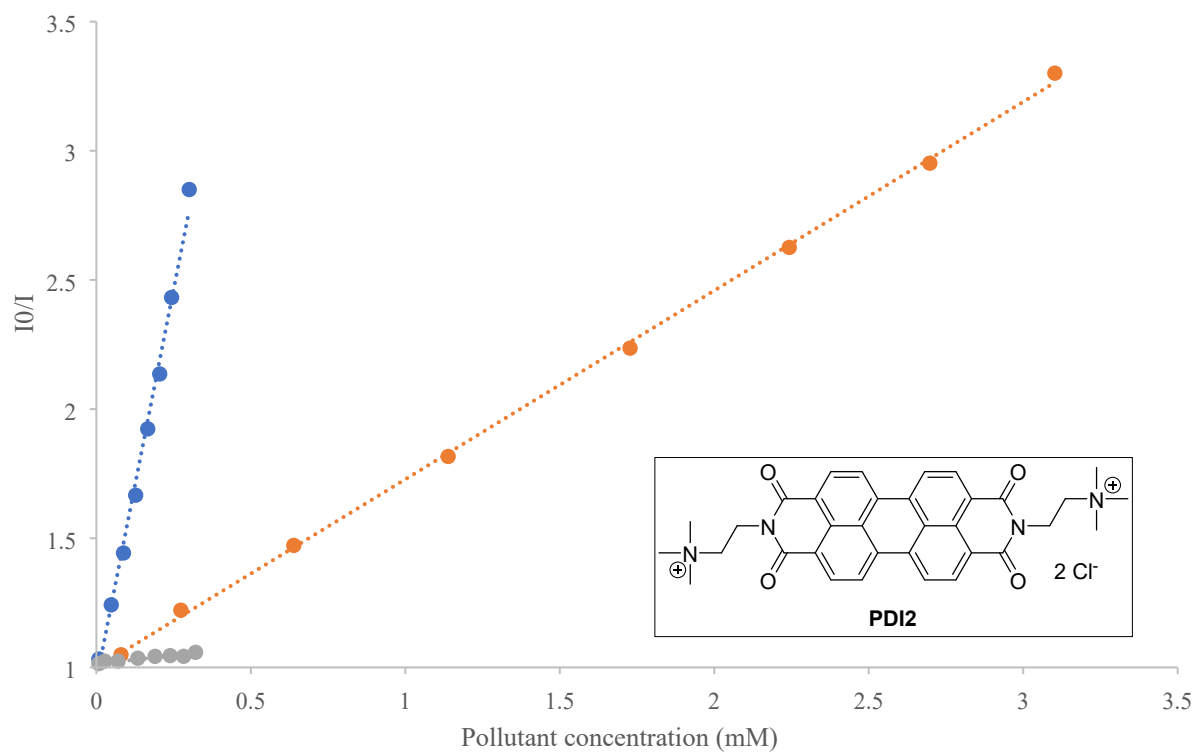


Figure S22. Stern Volmer plots with PDI2 in aqueous solution in presence of ofloxacin (orange line), diclofenac (blue line) and BPA (grey line). Inset: structure of PDI2.¹⁴

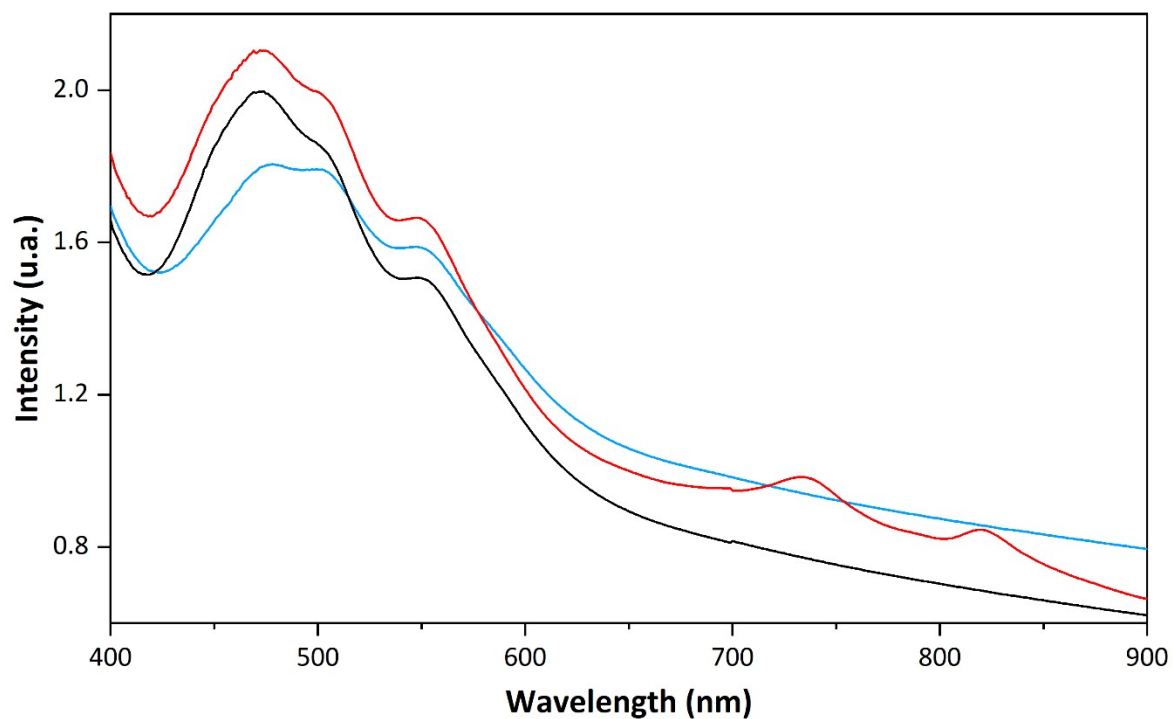


Figure S23. UV-Vis spectra of a suspension of PDI-SiO₂ in 1 mM ofloxacin (degassed) before (blue line) and after (red line) irradiation at 525 nm for 24h. Oxygenating the irradiated solution yields the black curve.

Table S4. Assignment of the remaining peaks on the chromatogram recorded after Fenton catalysis.

Peak retention time (mn)	M (Da)	Formula
4.68	224.1274	C ₉ H ₅ F ₅ O
	224.1273	C ₁₀ H ₁₆ N ₄ O ₂
	224.1272	C ₈ H ₄ N ₂ O ₆
	184.1335	C ₁₀ H ₁₇ NO ₂
3.93	210.1137	C ₁₁ H ₁₆ NO ₃
3.10	196.0959	C ₁₀ H ₁₄ NO ₃
1.11	173.0815	C ₆ H ₁₁ N ₃ O ₃

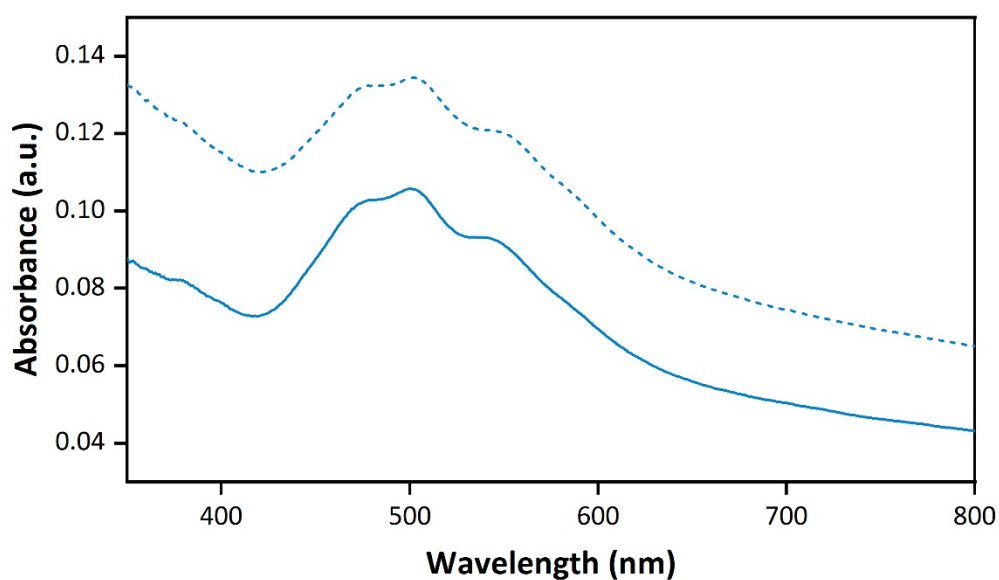


Figure S24. UV-Vis spectra of PDI-SiO₂ in water before (plain blue line) and after (dotted blue line) Fenton catalysis. Light scattering is responsible for the offset vs. the wavelength axis.

References

- 1 U. Schmidt, M. Weigert, C. Broaddus and G. Myers, 2018, vol. 11071, pp. 265–273.
- 2 D. Massiot, F. Fayon, M. Capron, I. King, S. Le Calvé, B. Alonso, J.-O. Durand, B. Bujoli, Z. Gan and G. Hoatson, *Magn. Reson. Chem.*, 2002, **40**, 70–76.
- 3 M. Thommes, K. Kaneko, A. V. Neimark, J. P. Olivier, F. Rodriguez-Reinoso, J. Rouquerol and K. S. W. Sing, *Pure Appl. Chem.*, 2015, **87**, 1051–1069.
- 4 M. Jaroniec, M. Kruk, J. P. Olivier and S. Koch, in *Studies in Surface Science and Catalysis*, eds. K. K. Unger, G. Kreysa and J. P. Baselt, Elsevier, 2000, vol. 128, pp. 71–80.
- 5 J. Font, P. de March, F. Busque, E. Casas, M. Benitez, L. Teruel and H. Garcia, *J. Mater. Chem.*, 2007, **17**, 2336–2343.
- 6 N. G. Tsierkezos, *J. Solut. Chem.*, 2007, **36**, 289–302.
- 7 V. V. Pavlishchuk and A. W. Addison, *Inorganica Chim. Acta*, 2000, **298**, 97–102.
- 8 Y. Shiraishi, S. Kanazawa, D. Tsukamoto, A. Shiro, Y. Sugano and T. Hirai, *ACS Catal.*, 2013, **3**, 2222–2227.
- 9 Y. Shiraishi, S. Kanazawa, Y. Sugano, D. Tsukamoto, H. Sakamoto, S. Ichikawa and T. Hirai, *Acs Catal.*, 2014, **4**, 774–780.
- 10 Y. Shiraishi, Y. Kofuji, H. Sakamoto, S. Tanaka, S. Ichikawa and T. Hirai, *ACS Catal.*, 2015, **5**, 3058–3066.
- 11 Y. Shiraishi, S. Kanazawa, Y. Kofuji, H. Sakamoto, S. Ichikawa, S. Tanaka and T. Hirai, *Angew. Chem. Int. Ed.*, 2014, **53**, 13454–13459.
- 12 Y. Pu, F. Bao, D. Wang, X. Zhang, Z. Guo, X. Chen, Y. Wei, J. Wang and Q. Zhang, *J. Environ. Chem. Eng.*, 2022, **10**, 107123.
- 13 S. Feng, Y.-P. Zhang, H. Xu, X. Gong and J. Hua, *J. Alloys Compd.*, 2023, **938**, 168500.
- 14 M. Gryszel, T. Schlossarek, F. Würthner, M. Natali and E. D. Głowacki, *ChemPhotoChem*, 2023, **7**, e202300070.